Journal of Materials Chemistry B

ROYAL SOCIETY OF CHEMISTRY

PAPER

View Article Online
View Journal | View Issue

Published on 20 December 2013. Downloaded by Montana State University Bozeman on 15/08/2014 22:14:55.

Cite this: J. Mater. Chem. B, 2014, 2, 1335

Synthesis and anticancer properties of phenyl benzoate derivatives possessing a terminal hydroxyl group

Yukako Fukushi,[a] Hironori Yoshino,[b] Junya Ishikawa,[b] Masanobu Sagisaka,[a] Ikuo Kashiwakura[b] and Atsushi Yoshizawa*[a]

Received 6th December 2013
Accepted 19th December 2013

DOI: 10.1039/c3tb21736a

www.rsc.org/MaterialsB

To assess the cytotoxic effects on A549 human lung cancer cells, we investigated a liquid-crystalline compound possessing a terminal hydroxyl group at concentrations of 0.1–20 μM. The compound, 4-butylphenyl 4-(6-hydroxyhexyloxy)benzoate (**2**), showed marked cell-growth inhibition at concentrations higher than 5 μM. Cell accumulation in the Sub-G1 phase indicating apoptosis was observed only at the highest concentration. Dynamic light scattering measurements show that the molecules form a spherical nanoparticle with a diameter of 130–170 nm at concentrations of 5–20 μM. We prepared the corresponding dimeric compounds and investigated their anticancer activity. The 1,2-benzene derivative, 1,2-bis[4-(6-hydroxyhexyloxy)benzoyloxy]benzene (**4**), exhibited cell-growth inhibition without affecting the cell cycle. However, the 1,3-benzene derivative, 1,3-bis[4-(6-hydroxyhexyloxy)benzoyloxy]benzene (**5**), was found to induce marked cell accumulation in the Sub-G1 phase. Furthermore, we assessed the cytotoxic effects of compounds **2**, **4** and **5** on SW480 colon cancer cells and THP1 leukemic cells, as well as on WI-38 normal fibroblast cells. Both compounds **2** and **5** suppressed the growth of the solid cancer cells (A549 and SW480) more strongly compared with that of the hematological cancer cells (THP1). Unexpectedly, they also exhibited a strong cytotoxicity against the normal cells. We discuss the structure–property relationship in the anticancer activity of the mesogenic compounds.

Introduction

Numerous studies have been conducted over the past few decades to develop effective anticancer agents either by synthesis or from natural products. Most chemotherapeutic drugs are classifiable as alkylating agents, antimetabolites, anthracyclines, plant alkaloids, topoisomerase inhibitors, monoclonal antibodies, molecular target drugs, or as other anticancer agents.[1–7] However, the development of anticancer agents against solid cancer cells such as lung cancer has presented some difficult problems. To reach cancer cells in optimal quantity, a therapeutic agent must pass through an imperfect blood vasculature to the cancer, cross the vessel walls into the interstitium, and penetrate multiple layers of solid cancer cells.[8,9] Furthermore, most anticancer drugs lack any intrinsic anticancer selectivity, thereby causing severe side effects because of the massive destruction of normal tissues. To overcome these hurdles, many drug carriers designed to deliver cytostatic agents exclusively at the tumor site have been investigated. Many strategies to entrap anticancer agents in different nanocarriers with a variety of architectures including polymer–drug conjugates,[10] micelles,[11] nanogels,[12] liposomes,[13] dendrimers,[14] and nanospheres[15,16] have been developed. Nanocarriers can be taken up by cells *via* endocytosis. The suitable size of such a nanocarrier for a tumor targeted by the enhanced permeability and retention (EPR) effect is known to be 100–200 nm.[17] In addition to these carriers, prodrug systems were designed.[18] The use of non-toxic prodrugs that can be activated by an enzyme that is naturally overexpressed in the tumor microenvironment has emerged as a promising strategy to enhance the selectivity of chemotherapy.

Biological systems have links with liquid crystallinity. Cell membranes are lamellar bilayer mesophases of phospholipids, glycolipids and cholesterol. Recently, we reported that some liquid-crystalline compounds induce cell-growth suppression in A549 lung cancer cells. Moreover, we described a relationship between anticancer activity and liquid-crystallinity.[19–21] We surmise that a supramolecular assembly consisting of liquid-crystalline molecules possessing a biologically active site is effective not only for cell permeability but also for cytotoxicity against tumor cells. On the other hand, various polyhydroxy compounds such as sugar derivatives and flavanol derivatives are known to show anticancer activity.[22,23] Conventional cyanobiphenyl derivatives possessing a primary alcohol showed

[a]Department of Frontier Materials Chemistry, Graduate School of Science and Technology, Hirosaki University, 3 Bunkyo-cho, Hirosaki, 036-8561, Japan. E-mail: ayoshiza@cc.hirosaki-u.ac.jp
[b]Department of Radiological Life Sciences, Hirosaki University Graduate School of Health Sciences, 66-1 Hon-cho, Hirosaki, Japan

Published on 20 December 2013. Downloaded by Montana State University Bozeman on 15/08/2014 22:14:55.

inhibition activity against A549 human lung cancer cells and did not exhibit suppressive effects on WI-38 normal fibroblast cells.[19] These lead to a design concept that molecular assembly of mesogenic compounds possessing a terminal hydroxyl group can induce aggregation of terminal alcohols exhibiting anticancer activities without severe side effects. Here, we investigated anticancer activities of some phenyl benzoate derivatives possessing a terminal hydroxyl group against A549 human lung cancer cells. Furthermore we designed the corresponding dimeric compounds, *i.e.*, 1,2- and 1,3-benzene derivatives with different configuration of their terminal hydroxyl groups and evaluated their anticancer activities.

Experimental

Characterization of materials

The purification of each final product was conducted using column chromatography over silica gel (63–210 nm; Kanto Chemical Co. Inc.) using a dichloromethane–ethyl acetate mixture as the eluent, followed by recrystallization from ethanol. The purity was confirmed using elemental analysis (EA 1110; CE Instruments Ltd.). The structures of the final products were elucidated using infrared (IR) spectroscopy (Varian 670-IR; Varian Inc.) and proton nuclear magnetic resonance (^{1}H NMR) spectroscopy (JNM-ECA 500; JEOL).

Preparation of materials

4-Butylphenyl 4-(6-hydroxyhexyloxy)benzoate (2). Ethyl 4-hydroxybenzoate (3.0 g, 18 mmol) and 6-bromo-1-hexanol were dissolved in cyclohexanone (15 ml). Potassium carbonate (5.0 g, 36 mmol) was then added. The resulting mixture was stirred at 110 °C for 10 h. The resulting mixture was filtered and the solvent was removed by evaporation under reduced pressure. The product was purified by column chromatography using a dichloromethane–ethyl acetate (10 : 1) mixture as the eluent. Recrystallization from hexane gave ethyl 4-(6-hydroxyhexyloxy)-benzoate. Yield: 3.4 g (71%).

Then, ethyl 4-(6-hydroxyhexyloxy)benzoate (530 mg, 2.0 mmol) was added to a solution of KOH (340 mg, 6.0 mmol) in ethanol (95%, 20 ml). The resulting mixture was stirred under reflux for 4 h. Next, water (40 ml) was added to the mixture. The solution was acidified with HCl (concentrated, 4.0 ml). The aqueous phase was extracted with dichloromethane (5 × 20 ml). The organic extracts were combined, dried over Na_2SO_4, filtered and evaporated. 4-(6-Hydroxyhexyloxy)benzoic acid was obtained. Yield: 0.34 g (71%).

4-(6-Hydroxyhexyloxy)benzoic acid (242 mg, 1.0 mmol), *N*,*N*′-dicyclohexylcarbodiimide (500 mg, 2.4 mmol) and 4-butylphenol (154 mg, 1.0 mmol) were added to dichloromethane (12 ml), and then 4-(*N*,*N*′-dimethylamino)pyridine (24 mg, 0.2 mmol) was added. The resulting solution was stirred at room temperature for 12 h. Then, the precipitated materials were removed by filtration. After removal of the solvent by evaporation, the residue was purified by column chromatography using a dichloromethane–ethyl acetate (10 : 1) mixture as the eluent. Recrystallization from ethanol gave the desired product. Yield: 150 mg (41%). ^{1}H NMR (500 MHz, solvent $CDCl_3$, standard TMS) δ_H/ppm: 8.14 (d, 2H, Ar-H, J = 9.2 Hz), 7.22 (d, 2H, Ar-**H**, J = 8.0 Hz), 7.10 (d, 2H, Ar-**H**, J = 8.6 Hz), 6.97 (d, 2H, Ar-**H**, J = 9.2 Hz), 4.06 (t, 2H, –OC**H**$_2$–, J = 6.6 Hz), 3.68 (t, 2H, –C**H**$_2$–OH, J = 6.6 Hz), 2.63 (t, 2H, Ar–C**H**$_2$–, J = 7.7 Hz), 1.85 (quin, 2H, –OCH$_2$C**H**$_2$–, J = 7.0 Hz), 1.66–1.45 (m, 8H, aliphatic –C**H**$_2$–), 1.38 (sext, 2H, –C**H**$_2$CH$_3$, J = 7.5 Hz), 1.28 (br s, 1H, –O**H**), 0.94 (t, 3H, –C**H**$_3$, J = 7.2 Hz). ν/cm^{-1} (KBr): 3360 (O–H str.), 2933, 2857 (C–H str.), 1725 (C=O str.), 1607, 1514 (C=C str.). Elemental analysis. Calculated for $C_{33}H_{40}O_8$: C, 74.56; H, 8.16. Found: C, 74.41; H, 8.05%.

1,2-Bis[4-(6-hydroxyhexyloxy)benzoyloxy]benzene (4). To a solution of catechol (110 mg, 1.0 mmol) in dichloromethane (10 ml), 4-(6-hydroxyhexyloxy)benzoic acid (480 mg, 2.0 mmol), *N*,*N*′-dicyclohexylcarbodiimide (500 mg, 2.4 mmol), and 4-(*N*,*N*′-dimethylamino)pyridine (240 mg, 4.0 mmol) were added. The resulting solution was stirred at room temperature for 12 h. Then, the precipitated materials were removed by filtration. After removal of the solvent by evaporation, the residue was purified by column chromatography using a dichloromethane–ethyl acetate (1 : 1) mixture as the eluent. Recrystallization from ethanol gave the desired product. Yield: 290 mg (52%). ^{1}H NMR (500 MHz, solvent $CDCl_3$, standard TMS) δ_H/ppm: 8.00 (d, 4H, Ar-**H**, J = 9.0 Hz), 7.37–7.31 (m, 4H, Ar-**H**), 6.83 (d, 4H, Ar-**H**, J = 8.9 Hz), 3.98 (t, 4H, –OC**H**$_2$–, J = 6.5 Hz), 3.66 (t, 4H, –C**H**$_2$–OH, J = 6.5 Hz), 1.81 (quin, 4H, –OCH$_2$C**H**$_2$–, J = 7.0 Hz), 1.61 (quin, 4H, –C**H**$_2$CH$_2$–OH, J = 7.0 Hz), 1.53–1.41 (m, 8H, aliphatic –C**H**$_2$–), 1.37 (br s, 2H, –O**H**). ν/cm^{-1} (KBr): 3317 (O–H str.), 2937, 2860 (C–H str.), 1737 (C=O str.), 1605, 1492 (C=C str.). Elemental analysis. Calculated for $C_{33}H_{40}O_8$: C, 70.19; H, 7.14. Found: C, 70.32; H, 6.80%.

1,3-Bis[4-(6-hydroxyhexyloxy)benzoyloxy]benzene (5). To a solution of resorcinol (110 mg, 1.0 mmol) in dichloromethane (10 ml), 4-(6-hydroxyhexyloxy)benzoic acid (480 mg, 2.0 mmol), *N*,*N*′-dicyclohexylcarbodiimide (500 mg, 2.4 mmol), and 4-(*N*,*N*′-dimethylamino)pyridine (240 mg, 4.0 mmol) were added. The resulting solution was stirred at room temperature for 6 h. Then, the precipitated materials were removed by filtration. After removal of the solvent by evaporation, the residue was purified by column chromatography using a dichloromethane–ethyl acetate (1 : 1) mixture as the eluent. Recrystallization from ethanol gave the desired product. Yield: 350 mg (63%). ^{1}H NMR (500 MHz, solvent $CDCl_3$, standard TMS) δ_H/ppm: 8.13 (d, 4H, Ar-**H**, J = 8.7 Hz), 7.45 (t, 1H, Ar-**H**, J = 8.2 Hz), 7.16–7.13 (m, 3H, Ar-**H**), 6.96 (d, 4H, Ar-**H**, J = 8.8 Hz), 4.05 (t, 4H, –OC**H**$_2$–, J = 6.5 Hz), 3.68 (q, 4H, –C**H**$_2$–OH, J = 6.2 Hz), 1.85 (quin, 4H, –OCH$_2$C**H**$_2$–, J = 7.0 Hz), 1.63 (quin, 4H, – C**H**$_2$CH$_2$–OH, J = 7.0 Hz), 1.55–1.44 (m, 8H, aliphatic –C**H**$_2$–), 1.26–1.23 (br m, 2H, –O**H**). ν/cm^{-1} (KBr): 3378 (O–H str.), 2934, 2859 (C–H str.), 1731 (C=O str.), 1606, 1512 (C=C str.). Elemental analysis. Calculated for $C_{33}H_{40}O_8$: C, 70.19; H, 7.14. Found: C, 70.21; H, 6.87%.

1,4-Bis-[4-(6-hydroxyhexyloxy)benzoyloxy]benzene (6). To a solution of hydroquinone (94 mg, 0.9 mmol) in dichloromethane (10 ml), 4-(6-hydroxyhexyloxy)benzoic acid (430 mg, 1.8 mmol), *N*,*N*′-dicyclohexylcarbodiimide (370 mg, 1.8 mmol), and 4-(*N*,*N*′-dimethylamino)pyridine (22 mg, 0.18 mmol) were added. The resulting solution was stirred at room temperature for 10 h. Then, the precipitated materials were removed by

 This journal is © The Royal Society of Chemistry 2014

Published on 20 December 2013. Downloaded by Montana State University Bozeman on 15/08/2014 22:14:55.

filtration. After removal of the solvent by evaporation, the residue was purified by column chromatography using a dichloromethane–ethyl acetate (1 : 1) mixture as the eluent. Recrystallization from an ethanol–hexane (1 : 1) mixture gave the desired product. Yield: 126 mg (25%). ^{1}H NMR (500 MHz, solvent $CDCl_3$, standard TMS) δ_H/ppm: 8.15 (d, 4H, Ar-**H**, $J = 9.2$ Hz), 7.26 (s, 4H, Ar-**H**), 6.98 (d, 4H, Ar-**H**, $J = 9.1$ Hz), 4.06 (t, 4H, –OC**H**$_2$–, $J = 7.6$ Hz), 3.68 (q, 4H, –C**H**$_2$–OH, $J = 6.1$ Hz), 1.85 (quin, 4H, –OCH$_2$C**H**$_2$–, $J = 6.9$ Hz), 1.63 (quin, 4H, –C**H**$_2$CH$_2$–OH, $J = 7.0$ Hz), 1.54–1.45 (m, 8H, aliphatic –C**H**$_2$–), 1.24 (t, 2H, –O**H**, $J = 5.5$ Hz). ν/cm^{-1} (KBr): 3402 (O–H str.), 2937, 2857 (C–H str.), 1730 (C=O str.), 1608, 1511 (C=C str.). Elemental analysis. Calculated for $C_{33}H_{40}O_8$: C, 70.19; H, 7.14. Found: C, 70.26; H, 6.85%.

Liquid-crystalline and physical properties

The initial assignments and corresponding transition temperatures for the final product were determined by thermal optical microscopy using a Nikon Optiphoto-pol polarizing microscope equipped with a Mettler FP82 hot stage and an FP80 control processor. The heating and cooling rates were 5 °C min^{-1}. Transition temperatures were investigated by differential scanning calorimetry (DSC) using a Seiko Instruments Inc. DSC6200. The materials were studied at a scanning rate of 5 °C min^{-1} after being encapsulated in aluminum pans. The lyotropic liquid crystallinity at 37 °C was determined by thermal optical microscopy using a polarizing microscope (BX-51, Olympus) equipped with a thermal stage (TS62, INSTEC), and a temperature controller (STC200, INSTEC). Each compound was dissolved in DMSO at a concentration of 10 mM. The DMSO solution was added to a suitable amount of water. Dynamic light scattering measurements were performed on an Otsuka Electronics FDLS-3000L equipped with a He–Ne laser beam at a wavelength of 632.8 nm at 37 °C. The scattering angle was fixed at 90°.

Cell line

To evaluate the anticancer activity of some liquid-crystalline compounds, an A549 human lung cancer cell line, a THP1 human leukemic cancer cell line and an SW480 human colon cancer cell line were selected. To investigate the toxicity on normal cells, we used a WI-38 normal fibroblast cell line. A549, THP1 and WI-38 cell line was purchased from the RIKEN Bio-Resource Center (Tsukuba, Japan), and SW480 cell lines were purchased from the American Type Culture Collection (Rockville, MD, USA). Briefly, each cell line was cultured in appropriate liquid culture medium including 1% penicillin/streptomycin and 10% heat-inactivated fetal bovine serum (Bioserum, UBC, Japan) as shown in Table 1.

Cell growth inhibition assay

Each evaluated compound was dissolved in dimethyl sulfoxide (Wako, Osaka, Japan, DMSO) at a concentration of 10 mM. Each cell line (A549: 4×10^3 cells per ml, THP1: 5×10^4 cells per ml, SW480: 4×10^3 cells per ml, WI-38: 4×10^3 cells per ml) was placed at 1 or 0.5 ml per well in 24-well plates at 37 °C in a humidified atmosphere with 5% CO_2. After 24 h incubation, A549, SW480 and WI-38 cells were refed with fresh medium supplemented with each compound. After culturing (A549: 96 h, SW480: 96 h, WI-38: 168 h), cells attached to the plates were released by trypsinization, and cell count was confirmed by the trypan blue dye exclusion test. However, since some SW480 cells were floating in solvent (DMSO)-treated control, not only cells attached to the plates but also floating cells were harvested. With respect to THP1, each compound was added to the culture immediately after seeding the cells. After 72 h culturing, THP1 cells were harvested, and cell count was performed. Cell viability was expressed as a percentage relative to solvent (DMSO)-treated control incubations.

Table 1 Cell lines, cell type and culture medium

Cell line	Cell type	Culture medium[a]
A549	Lung	DMEM
SW480	Colon	RPMI1640
THP 1	Leukemia	RPMI1640
WI-38	Fibroblast	MEME

[a] DMEM: Dulbecco's MEM (Gibco®, Invitrogen Corp., California, USA), RPMI: Roswell Park Memorial Institute (Gibco®, Invitrogen Corp., California, USA), MEME: Minimum essential medium eagle (Sigma-Aldrich, Japan).

Cell cycle analysis

A549 cells (3×10^3 cells per ml) were placed in a 60 mm dish (IWAKI, Tokyo, Japan) at 37 °C in a humidified atmosphere with 5% CO_2. After 24 h incubation, cells were refed with fresh medium supplemented with each compound. After 24 and 48 h of treatment, cells were washed with phosphate-buffered saline (PBS). Then, cells attached to the plates were released by trypsinization, and cell count was confirmed by the trypan blue dye exclusion test. The harvested A549 cells (3×10^5 cells per ml) were washed with PBS and fixed with 70% ethanol for more than 24 h. The fixed cells were washed with PBS and then treated with RNase (200 μg ml^{-1}) at 37 °C for 30 min. After treatment, the cells were washed with PBS, and stained with 25 μg ml^{-1} propidium iodide (Sigma, Tokyo, Japan, PI) for 30 min at room temperature in the dark. The cell cycle distribution was analyzed using a Cytomics FC500 (Beckman-Coulter, Fullerton, CA, USA).

Statistical analysis

A test to reject outliers was conducted for results obtained using the cell proliferation assay. Outliers were dismissed by a 5% level. Significant differences between the control and the experimental groups were determined using Mann–Whitney's *U*-test.

Results and discussion

Synthesis and biological activities of phenyl benzoate derivatives

We prepared phenyl benzoate derivatives **1–3** and evaluated their cytotoxicity against A549 human lung cancer cells. Their molecular structures are shown in Fig. 1. Compounds **1** and **2**

Published on 20 December 2013. Downloaded by Montana State University Bozeman on 15/08/2014 22:14:55.

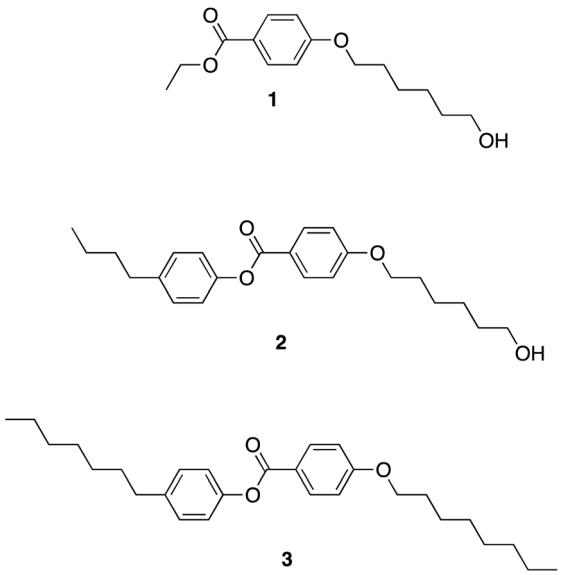

Fig. 1 Molecular structures of compounds **1–3**.

were prepared by a synthetic method as depicted in Scheme 1. Both compounds were purified by column chromatography and then by recrystallization from ethanol. Compound **3**[24] was prepared using a method similar to that described in Scheme 1.

The cell viability of A549 cells was estimated by treatment with each compound at 10 μM for 96 h. The cell-growth inhibition ratio was 0% for compound **1**, 99% for compound **2** and 20% for compound **3**, as presented in Fig. 2. Compound **2** showed marked inhibition of the cell proliferation compared to the other compounds, indicating that both a phenyl benzoate unit and a terminal hydroxyl group contribute to the cell inhibition. We observed the dose-dependent cytotoxicities of compound **2** on A549 lung cancer cells. The results are depicted in Fig. 3. The cell viability decreases with increasing concentrations of compound **2**. The 50% inhibitory concentration (IC_{50}) for 96 h was 4.7 μM.

One characteristic of cancer cells is their uncontrolled growth by mutation or deregulation of cell cycle checkpoints. To clarify the origin of cell suppression, we investigated the inhibition effects of compound **2** on the cell cycle profile in A549 cell proliferation. The A549 lung cancer cells were treated with compound **2** (10 μM and 20 μM). The cell cycle profiles were

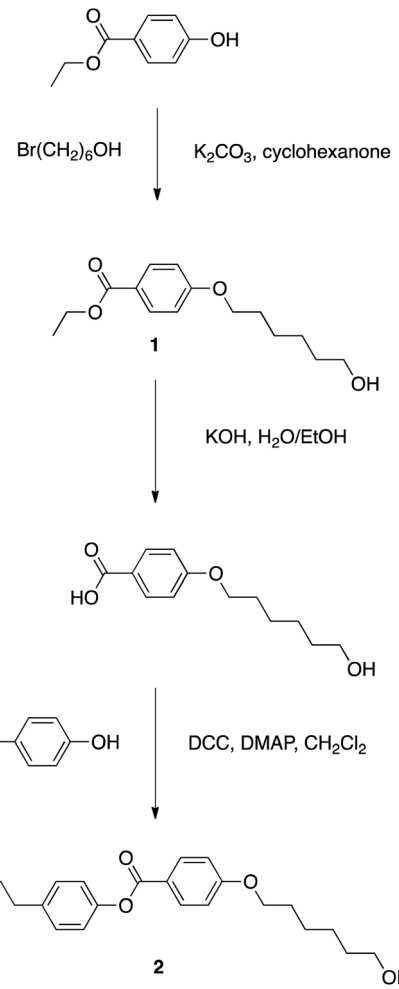

Scheme 1 Synthesis of phenyl benzoate derivatives **1** and **2**.

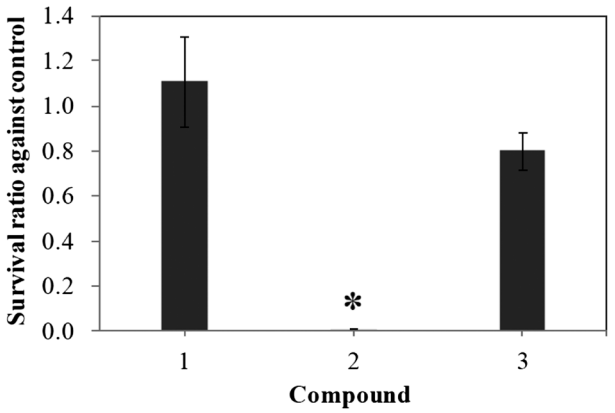

Fig. 2 Effects of compounds **1–3** on human lung carcinoma A549 cell growth at a concentration of 10 μM for 96 h. *$p < 0.05$ by Mann–Whitney's *U*-test.

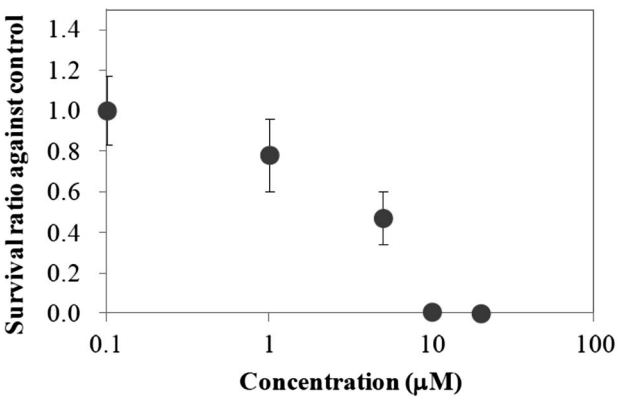

Fig. 3 Dose-dependent cytotoxicities of compound **2** on A549 cells for 96 h.

This journal is © The Royal Society of Chemistry 2014

Published on 20 December 2013. Downloaded by Montana State University Bozeman on 15/08/2014 22:14:55.

analyzed using flow cytometry. Fig. 4(a) shows the cell cycle distributions for 24 h and those for 48 h including both adherent cells and floating cells. As a result, compound **2** was found to induce cell accumulation in the Sub-G1 phase at a concentration of 20 μM. The cell accumulations in the Sub-G1 phase were 33% for 24 h and 61% for 48 h, whereas those for the control were less than 1%. The inhibition ratios of compound **2** were 62% for 24 h and 88% for 48 h. On the other hand, with a concentration of 10 μM, no significant difference was found in the cell cycle distribution between the control and compound **2**.

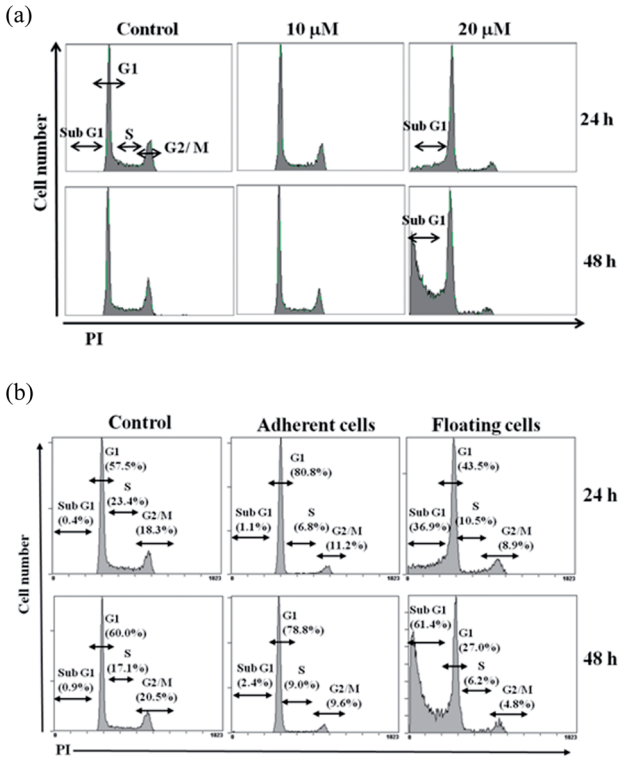

Fig. 4 (a) Dose-dependent effects of compound **2** on the cell cycle distribution in A549 lung cancer cells. (b) Cell cycle distribution in adherent cells and that in floating cells in the presence of compound **2** at a concentration of 20 μM.

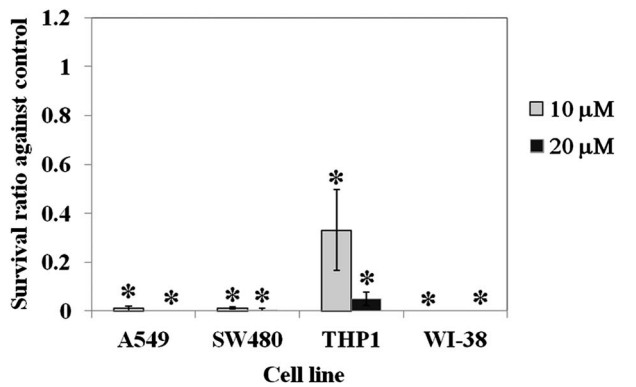

Fig. 5 Effects of compound **2** on cell proliferation of A549 lung cancer cells, SW480 colon cancer cells, THP1 leukemic cells and WI-38 normal fibroblast cells at 10 μM and 20 μM. Those cells cultured in the presence of compound **2** were harvested (A549: 96 h, SW480: 96 h, THP1: 72 h, WI-38: 168 h). Survivor cells were not detected in A549 cells in the presence of compound **2** at 20 μM. They were not detected in WI-38 cells in the presence of compound **2** at 10 μM and 20 μM. *$p < 0.05$ by Mann–Whitney's *U*-test.

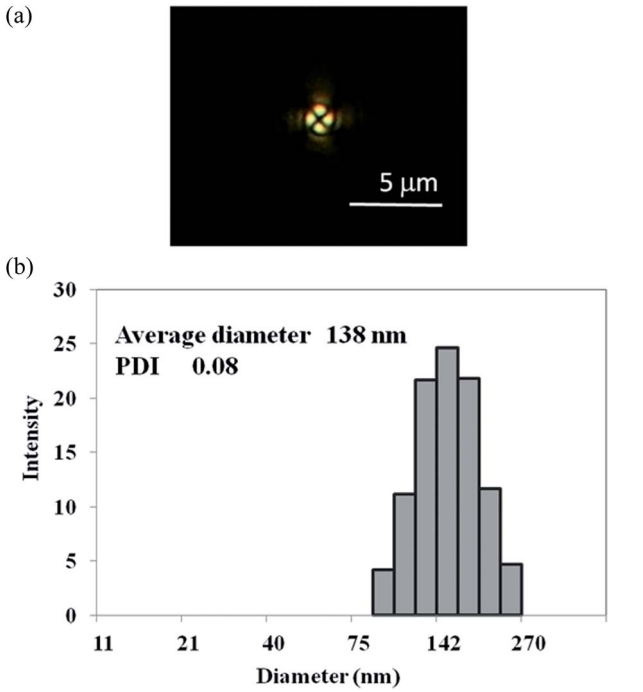

Fig. 6 (a) Photomicrograph of compound **2** at 100 μM in DMSO–H_2O (1 : 99) solution at 37 °C under crossed polarizers. (b) Dynamic light scattering profile of the aggregation system of compound **2** at 10 μM in DMSO–H_2O (1 : 999) solution at 37 °C.

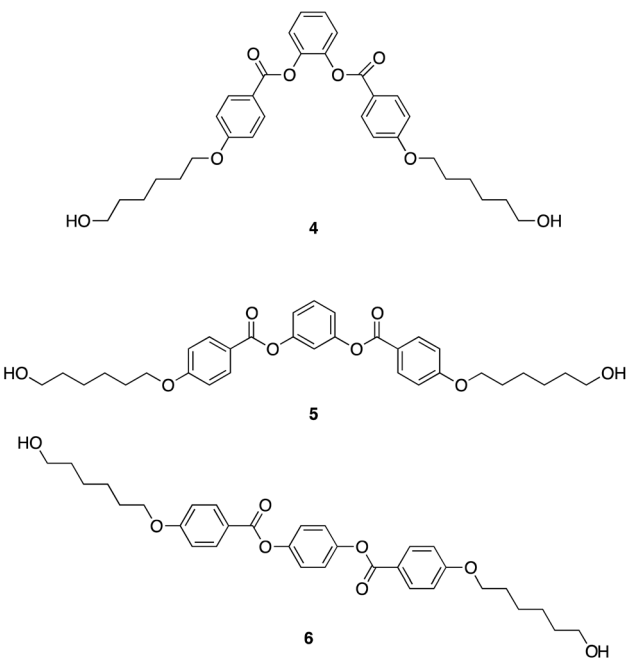

Fig. 7 Molecular structures of compounds **4**, **5** and **6**.

Published on 20 December 2013. Downloaded by Montana State University Bozeman on 15/08/2014 22:14:55.

The inhibition ratios of compound **2** at 10 μM were 32% for 24 h and 41% for 48 h. The results shown in Fig. 4(a) are the cell cycle distributions including both adherent cells and floating cells. In order to clear whether the cell accumulation in the Sub-G1 phase is induced in adherent cells or floating cells, effects of compound **2** at a concentration of 20 μM for 24 h on the cell cycle distribution were evaluated separately in adherent cells and in floating cells (Fig. 4(b)). With respect to the adherent cells, the cell accumulation increases in the G1 phase compared with the control, whereas there is no significant difference in cell accumulation in the Sub-G1 phase between them. With respect to the floating cells, the cell accumulation in the G1 phase decreases whereas that in the Sub-G1 phase increases markedly. Therefore, compound **2** is thought to induce programmed apoptosis following G1 arrest in A549 lung cancer cells. On the other hand, the cyanobiphenyl derivatives possessing a terminal alcohol did not induce cell death.[19] The phenyl benzoate unit plays an important role in the cytotoxicity of compound **2**.

We evaluated the cytotoxicity of compound **2** against the other tumor cells, SW480 colon cancer cells and THP1 leukemic cells, as well as WI-38 normal fibroblast cells. Fig. 5 shows effects of compound **2** on the growth of those cell lines at a concentration of 10 μM and 20 μM. Compound **2** exhibits a marked cell-growth inhibition against SW480 colon cells at a concentration of 10 μM. Although it also shows cytotoxicity against THP1 leukemic cancer cells, cell-growth inhibition of the cancer cells is much smaller than that of the solid cancer cells (A549 and SW480). These results suggest that compound **2** tends to suppress the growth of solid cancer cells more strongly compared with that of hematological cancer cells. Unexpectedly, compound **2** exhibited a strong cytotoxicity against WI-38 normal fibroblast cells, indicating that it has severe side effects.

We evaluated the ability of molecular aggregation for compound **2**. We observed thermotropic phase transition behaviour of compound **2** using polarized optical microscopy and DSC. On cooling, compound **2** exhibited an isotropic to nematic phase transition at 57.1 °C. Its melting point was 64.5 °C. We then investigated the lyotropic liquid-crystallinity of compound **2**. Fig. 6(a) portrays a photomicrograph of compound **2** (100 μM) in DMSO–H_2O (1 : 99) solution at 37 °C under crossed polarizers. The maltase cross texture suggests that compound **2** forms a spherical molecular aggregation in DMSO–H_2O mixture solution. The texture was not confirmed by POM at a concentration lower than 100 μM because the texture size might be smaller than 1 μm. Therefore, we observed the formation of particles of compound **2** in DMSO–H_2O (1 : 999) solution using dynamic light scattering. Fig. 6(b) shows the histogram of compound **2** at 10 μM. The average diameter was 138 nm with a poly-dispersity index (PDI) value of 0.08. The formation of particles was confirmed at the other concentrations. The diameters were 166 nm at 5 μM with a PDI value of 0.06 and 134 nm at 20 μM with a PDI value of 0.07. However, we could not estimate the diameter at a concentration of 1 μM due

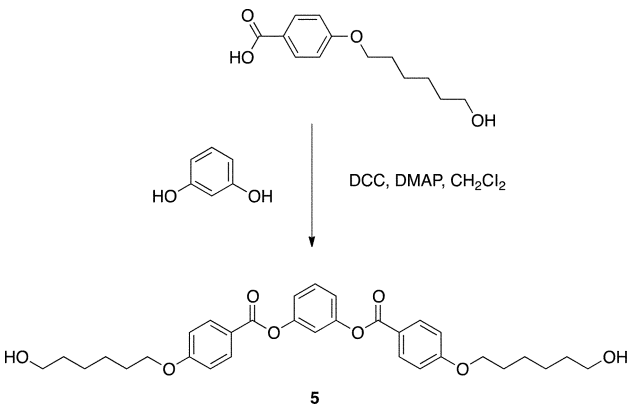

Scheme 2 Synthesis of compound **5**.

Table 2 Cell accumulation (%) in the Sub-G1 phase and the inhibition ratio (%) against control in brackets for compounds **4** and **5** for 96 h

	4		**5**	
	10 μM	20 μM	10 μM	20 μM
24 h	0.6 (21)	1.5 (41)	24.1 (52)	46.4 (56)
48 h	0.8 (34)	0.8 (60)	20.7 (81)	63.8 (93)

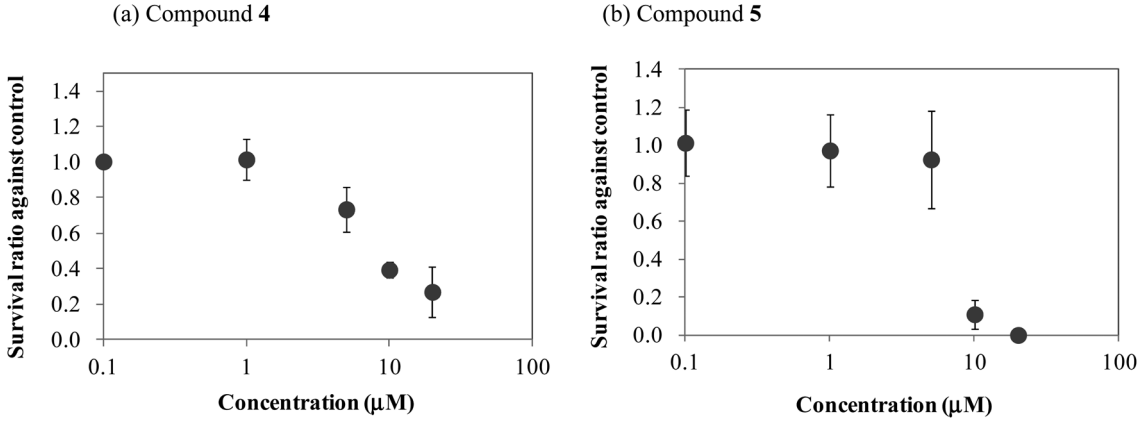

Fig. 8 Dose-dependent cytotoxicity of compound **4** and that of compound **5** on A549 cells for 96 h.

 This journal is © The Royal Society of Chemistry 2014

Published on 20 December 2013. Downloaded by Montana State University Bozeman on 15/08/2014 22:14:55.

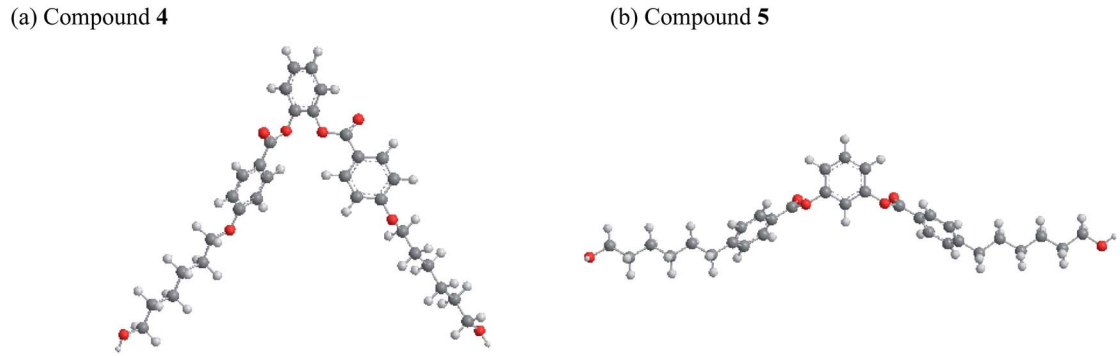

Fig. 9 MOPAC models for (a) compound 4 and (b) compound 5.

to a large experimental error. At least we can say that compound 2 forms a spherical molecular assembly possessing a suitable size for EPR effects[17] with a concentration range of 5–20 μM. The molecular assembly of compound 2 might be taken up by the cells *via* endocytosis. At present we do not have experimental evidence how the molecules penetrate multiple layers of the solid cancer cells. We cannot exclude the other penetration mechanism. There is marked dose-dependent effects of compound 2 on the cell distribution in A549 lung cancer cells, indicating that the intracellar interaction between compound 2 and a nucleus of the tumor depends on the concentration.

Synthesis and biological activities of compounds possessing two terminal hydroxyl groups

In order to know how compound 2 interacts with the nucleus, we designed some dimeric compounds, *i.e.*, 1,2-, 1,3- and 1,4-benzene derivatives with different configurations of their terminal hydroxyl groups (Fig. 7). The compounds were prepared by a synthesis outlined in Scheme 2.

We investigated the anti-proliferative activity of compounds 4 and 5 against A549 lung cancer cells. Unfortunately, 1,4-derivative 6 could not be tested because of the low solubility in the culture. Fig. 8 shows the dose-dependent suppressive effects. The anti-proliferative activity of compound 4 increases continuously with increasing concentrations, whereas that of compound 5 shows a discontinuous increase from 5 μM to 10 μM. IC_{50} values of compounds 4 and 5 for 96 h were 5.8 μM and 8.9 μM, respectively. We investigated the effects of compounds 4 and 5 on the cell cycle profile in A549 cell proliferation. Table 2 presents the cell accumulation in the Sub-G1 phase and the inhibition ratios for compounds 4 and 5. No significant difference in the cell distribution was found between the control and compound 4. However, marked cell accumulation was observed in the Sub-G1 phase for compound 5, indicating that compound 5 induced cell death caused by DNA fragmentation. Compound 4 exhibits cell-growth inhibition without inducing cell death, which is similar to that observed for compound 2 at a concentration of 10 μM. On the other hand, compound 5 was found to induce marked cell accumulation in the Sub-G1 phase, which is similar to that observed for compound 2 at a concentration of 20 μM. Molecular structures are obtained by semi-empirical calculations using MOPAC-6/PM3, as presented in Fig. 9.

Compounds 4 and 5 can produce a significant difference in the mechanism of the cytotoxicity against A549 lung cancer cells. Compound 4 might interact with the nucleus *via* the hydroxyl groups whereas compound 5 might interact with it *via* both hydroxyl and ester groups. The structure–property relationship in anticancer activity indicates that compound 2

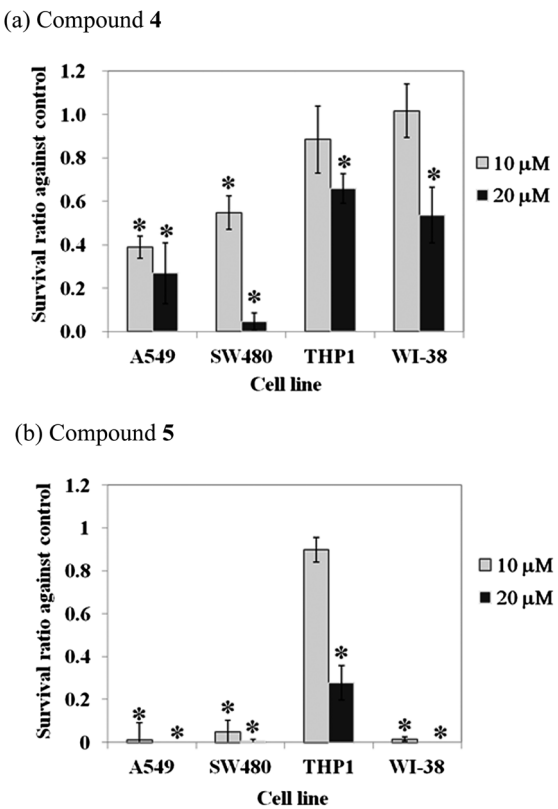

Fig. 10 Effects of compounds 4 and 5 on cell proliferation of A549 lung cancer cells, SW480 colon cancer cells, THP1 leukemic cells and WI-38 normal fibroblast cells at 10 μM and 20 μM. Those cells cultured in the presence of each compound were harvested (A549: 96 h, SW480: 96 h, THP1: 72 h, WI-38: 168 h). Survivor cells were not detected in A549 and WI-38 cells in the presence of compound 5 at a concentration of 20 μM. *$p < 0.05$ by Mann–Whitney's *U*-test.

Published on 20 December 2013. Downloaded by Montana State University Bozeman on 15/08/2014 22:14:55.

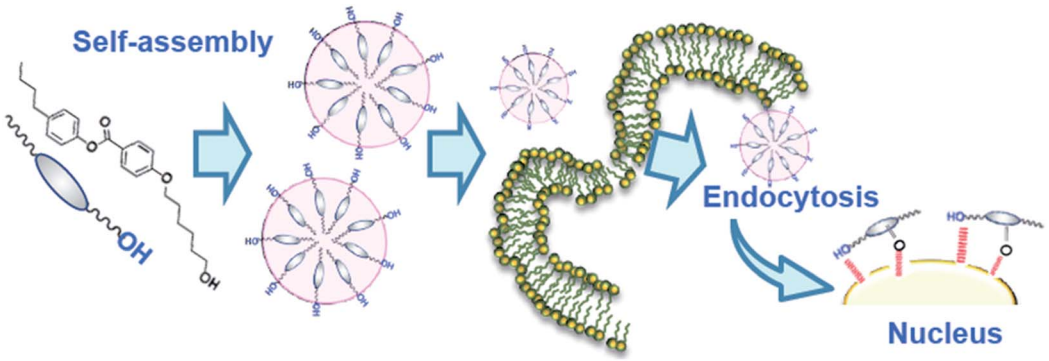

Fig. 11 Schematic illustration of a mechanism for cytotoxic effects of liquid-crystalline compound **2** against A549 lung cancer cells.

interacts with the nucleus *via* the hydroxyl and ester groups and induces cell death in A549 lung cancer cells at a concentration of 20 μM.

We evaluated their cytotoxicities against SW480 colon cancer cells, THP1 leukemic cells and WI-38 normal fibroblast cells. Fig. 10 shows the effects of compounds **4** and **5** on cell-growth inhibition of those cells. Compound **4** shows much smaller cell-growth inhibition against those cells than compounds **2** and **5**. On the other hand, compound **5** was found to suppress not only the proliferation of SW480 colon cancer cells but also that of WI-38 normal fibroblast cells at 10 μM, similarly to compound **2**.

The structure–property relationship in anticancer activity suggests the following mechanism for the cytotoxic effects of compound **2** against A549 lung cancer cells (Fig. 11): (1) self-assembly of the molecules produces spherical nanoparticles with a suitable size for EPR effects, (2) the nanoparticles might be taken up by the cells *via* endocytosis, and (3) the molecules might interact with the nucleus *via* the hydroxyl group at a concentration lower than 10 μM whereas they might interact with it *via* the hydroxyl and ester groups at 20 μM. Unexpected cytotoxicity of compound **2** against WI-38 normal fibroblast cells is thought to be attributed to not only the terminal alcohol but also the ester group interacting with the nucleus.

Conclusion

Liquid-crystalline compound **2** possessing a phenyl benzoate unit and a terminal hydroxyl group exhibited cytotoxicity on A549 lung cancer cells with an IC_{50} value of 4.7 μM. Compound **2** formed a spherical molecular assembly with a suitable diameter for EPR effects. Although no difference in cell cycle distribution was found between the control and compound **2** at 10 μM, induction of cell death through cell cycle arrest in the G1 phase of A549 cells was observed for compound **2** at a concentration of 20 μM, indicating that compound **2** has potential to induce programmed apoptosis in A549 lung cancer cells. Unexpectedly, compound **2** showed cytotoxicity against WI38 normal fibroblast cells. We designed some dimeric compounds possessing two terminal hydroxyl groups. 1,2-Disubstituted benzene derivative **4** showed cell-growth inhibition without affecting the cell cycle distribution similarly to compound **2** at a concentration of 10 μM. On the other hand, 1.3-disubstituted benzene derivative **5** induced cell death through cell cycle arrest in the G1 phase similarly to compound **2** at a concentration of 20 μM. We propose a mechanism of cytotoxic effects of compound **2** against A549 lung cancer cells as follows: (1) the liquid-crystalline molecules organize into a spherical particle with a suitable size for EPR effects, (2) the particles can be taken up by the cells *via* endocytosis, and (3) the molecules interact with the nucleus *via* the hydroxyl and ester groups to induce cell death.

Acknowledgements

This work was supported by a Grant-in-Aid for Scientific Research (no. 25107702) on the Innovative Areas: "Fusion Materials" (Area no. 22006) from MEXT.

Notes and references

1 P. L. Kuo, Y. L. Hsu, T. C. Lin and J. K. Chang, *Anti-Cancer Drugs*, 2005, **4**, 409.
2 A. Abe, M. Yamane and A. Tomoda, *Anti-Cancer Drugs*, 2001, **12**, 377.
3 K. Skobridis, M. Kinigopoulou, V. Theodrou, E. Giannousi, A. Russell, R. Chauhan, R. Sala, N. Brownlow, S. Kiriakdis, J. Domin, G. A. Tzakos and N. J. Dibb, *ChemMedChem*, 2010, **5**, 130.
4 J. H. Chang, C. F. Hung, S. C. Yang, J. P. Wang, S. J. Won and C. N. Lin, *Bioorg. Med. Chem.*, 2008, **16**, 7270.
5 A. Goel, A. K. Prasad, V. S. Parmar, B. Ghosh and N. Saini, *FEBS Lett.*, 2007, **581**, 2447.
6 T. C. Chou, X. Zhang, Z. Y. Zhong, Y. Li, L. Feng, S. Eng, D. R. Myles, R. Johnson, N. Wu, Y. I. Yin, R. M. Wilson and S. J. Danishefsky, *Proc. Natl. Acad. Sci. U. S. A.*, 2008, **35**, 13157.
7 J. H. Zhang, C. D. Fan, B. X. Zhao, D. S. Shin, W. L. Dong, Y. S. Xie and J. Y. Miao, *Bioorg. Med. Chem.*, 2008, **16**, 10165.
8 A. J. Primeau, A. Rendon, D. Hedley, L. Lilge and I. F. Tannock, *Clin. Cancer Res.*, 2005, **11**, 8782.
9 J. Lankelma, H. Dekker, R. F. Luque, S. Luykx, K. Hoekman, P. van der Valk, P. J. van Diest and H. M. Pinedo, *Clin. Cancer Res.*, 1999, **5**, 1703.

 This journal is © The Royal Society of Chemistry 2014

Published on 20 December 2013. Downloaded by Montana State University Bozeman on 15/08/2014 22:14:55.

10 S. F. Yu, Z. Wang, G. L. Wu, Y. N. Wang, H. Gao and J. B. Ma, *Acta Polym. Sin.*, 2012, **4**, 427.
11 J. Wang, Y. Wang and W. Liang, *J. Controlled Release*, 2012, **160**, 637.
12 J. Ding, F. Shi, C. Xiao, L. Lin, L. Chen, C. He, X. Zhuang and X. Chen, *Polym. Chem.*, 2011, **2**, 2857.
13 A. A. Gabizon, D. Tzemach, A. T. Horowitz, H. Shmeeda, J. Yeh and S. Zalipsky, *Clin. Cancer Res.*, 2006, **12**, 1913.
14 J. Hu, Y. Su, H. Zhang, T. Xu and Y. Cheng, *Biomaterials*, 2011, **32**, 9950.
15 J. You, R. Zhang, C. Xiong, M. Zhong, M. Melancon, S. Gupta, A. M. Nick, A. K. Sood and C. Li, *Cancer Res.*, 2012, **72**, 4777.
16 N. Tang, G. Du, N. Wang, C. Liu, H. Hang and W. Liang, *J. Natl. Cancer Inst.*, 2007, **99**, 1004.
17 K. Murayama, *Adv. Drug Delivery Rev.*, 2011, **63**, 161.
18 M. Grinda, J. Clarhaut, B. Renoux, I. T. Opalinski and S. Papot, *Med. Chem. Commun.*, 2012, **3**, 6870.
19 A. Yoshizawa, Y. Takahashi, A. Nishizawa, K. Takeuchi, M. Sagisaka, K. Takahashi, M. Hazawa and I. Kashiwakura, *Chem. Lett.*, 2009, **38**, 530.
20 Y. Takahashi, M. Hazawa, K. Takahashi, M. Sagisaka, I. Kashiwakura and A. Yoshizawa, *Med. Chem. Commun.*, 2011, **2**, 55.
21 Y. Takahashi, M. Hazawa, K. Takahashi, A. Nishizawa, A. Yoshizawa and I. Kashiwakura, *Invest. New Drugs*, 2011, **29**, 659.
22 L. Actis-Goretta, L. J. Romanczyk, C. A. Rodriguez, C. Kwik-Uribe and C. L. Keen, *J. Nutr. Biochem.*, 2008, **19**, 797.
23 M. Jung, Y. Lee, H.-I. Moon, Y. Jung, H. Jung and M. Oh, *Eur. J. Med. Chem.*, 2009, **44**, 3120.
24 J. D. Margerum, S.-M. Wong, A. M. Lackner, J. E. Jensen and S. A. Verzwyvelt, *Mol. Cryst. Liq. Cryst.*, 1982, **84**, 79.